# Performance of the Resistive Plate Chambers in the CMS experiment

Filip Thyssen
for the CMS Collaboration

2011.09.14

# Outline

# Outline

1. The Compact Muon Solenoid Experiment
   - Large Hadron Collider
   - Compact Muon Solenoid
   - Muon Subdetectors
   - Resistive Plate Chambers
2. RPC Detector Performance
   - Hit Efficiencies
   - Hit Resolutions
   - High Voltage Scan and Results
3. RPC Trigger Performance
   - CMS Trigger system
   - RPC Pattern Comparator
4. Background studies
5. Conclusions

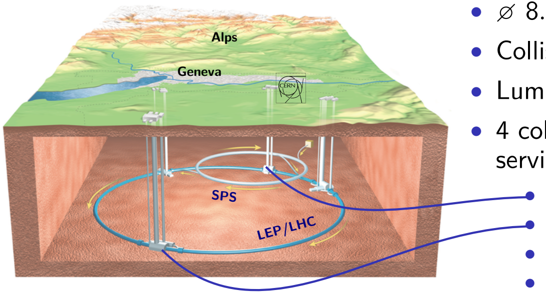


- $\varnothing$ 8.6 km p-p collider
- Collisions at $\sqrt{s} = 7\,\text{TeV}$
- Luminosity $\approx 10^{33}\,\text{cm}^{-2}\,\text{s}^{-1}$
- 4 collision points serving 6 experiments
  - ATLAS
  - CMS
  - ALICE
  - LHCb
  - LHCf
  - TOTEM

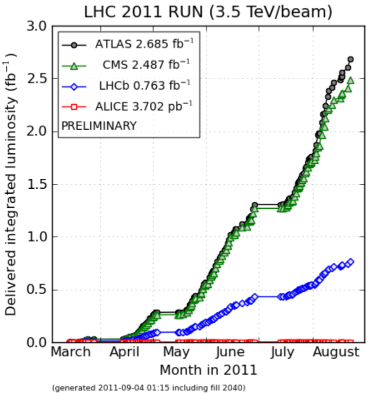


- $\varnothing$ 8.6 km p-p collider
- Collisions at $\sqrt{s} = 7\,\text{TeV}$
- Luminosity $\approx 10^{33}\,\text{cm}^{-2}\,\text{s}^{-1}$
- 4 collision points serving 6 experiments
  - ATLAS
  - CMS
  - ALICE
  - LHCb
  - LHCf
  - TOTEM

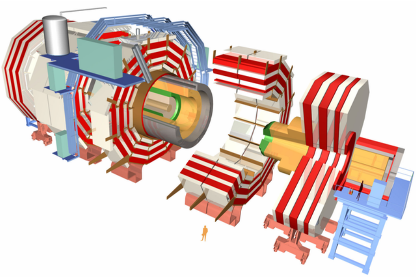

Compact Muon Solenoid

12 500 t, 21.6 m long, ⌀ 15 m

- Pixel and MicroStrip tracker

  Silicon, $75 \times 10^6$ channels

- Electromagnetic Calorimeter

  Scintillating $PbWO_4$ crystals

- Hadronic Calorimeter

  Plastic scintillator / brass

- SuperConducting Solenoid

  3.8 T magnetic field

- Muon Subdetectors

  $\Delta p_T / p_T \sim 5\%$ at 1 TeV/c

- Iron return yoke

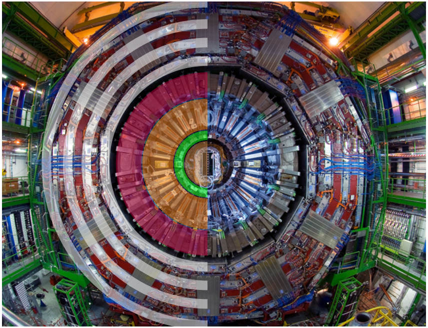

Compact Muon Solenoid

12 500 t, 21.6 m long, ⌀ 15 m

- Pixel and MicroStrip tracker

  Silicon, $75 \times 10^6$ channels

- Electromagnetic Calorimeter

  Scintillating $PbWO_4$ crystals

- Hadronic Calorimeter

  Plastic scintillator / brass

- SuperConducting Solenoid

  3.8 T magnetic field

- Muon Subdetectors

  $\Delta p_T / p_T \sim 5\%$ at 1 TeV/c

- Iron return yoke

# The Compact Muon Solenoid Experiment

## The Muon Subdetectors

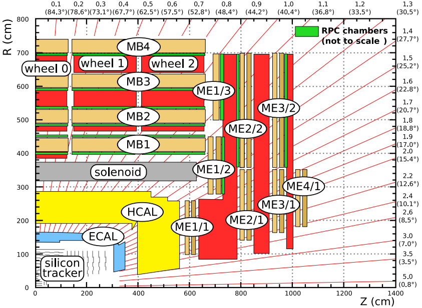


- 3 gaseous particle detector technologies
- Cylindrical barrel region
  - MB: Muon Barrel
  - 4 coaxial stations interleaved with iron return yokes
  - Drift Tubes and Resistive Plate Chambers
- Planar endcap regions
  - ME: Muon Endcap
  - 4 planar stations interleaved with iron return yokes
  - Cathode Strip Chambers and Resistive Plate Chambers

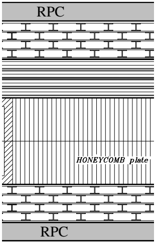


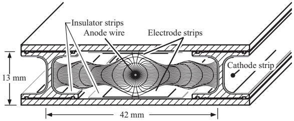


- 250 Drift Tube Chambers
  - Barrel region $|\eta| < 1.2$
  - 4 stations, 5 wheels, 12 sectors
  - $(4 + 4)$ layers measuring $\phi$
  - 4 layers measuring $z$ in stations 1-3
  - Local segment per chamber
  - Spatial resolution $\sim 250\,\mu\text{m}$

# The Compact Muon Solenoid Experiment

## The Muon Subdetectors

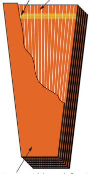


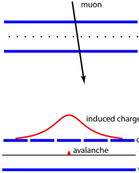


- 250 Drift Tube Chambers
  - Barrel region $|\eta| < 1.2$
  - 4 stations, 5 wheels, 12 sectors
  - $(4+4)$ layers measuring $\phi$
  - 4 layers measuring $z$ in stations 1-3
  - Local segment per chamber
  - Spatial resolution $\sim 250\,\mu\text{m}$
- 540 Cathode Strip Chambers
  - Endcap Region $0.9 < |\eta| < 2.4$
  - $2 \times 4$ stations, $1-3$ rings, $18-36$ sectors
  - 6 layers of strips per chamber measuring $\phi$
  - 6 layers of anode wires per chamber measuring $r$
  - Local segment per chamber
  - Spatial resolution $\sim 150\,\mu\text{m}$

# The Compact Muon Solenoid Experiment

## The Muon Subdetectors

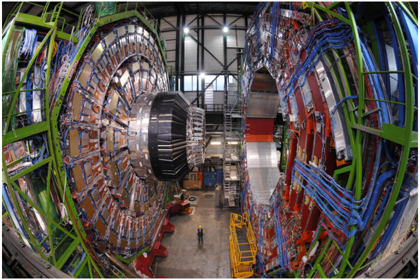

- 250 Drift Tube Chambers
  - Barrel region $|\eta| < 1.2$
  - 4 stations, 5 wheels, 12 sectors
  - $(4+4)$ layers measuring $\phi$
  - 4 layers measuring $z$ in stations 1-3
  - Local segment per chamber
  - Spatial resolution $\sim 250\,\mu m$
- 540 Cathode Strip Chambers
  - Endcap Region $0.9 < |\eta| < 2.4$
  - $2 \times 4$ stations, $1-3$ rings, $18-36$ sectors
  - 6 layers of strips per chamber measuring $\phi$
  - 6 layers of anode wires per chamber measuring $r$
  - Local segment per chamber
  - Spatial resolution $\sim 150\,\mu m$
- $480 + 432$ Resistive Plate Chambers
  - Both regions, $|\eta| < 1.6$
  - Barrel: 4 stations, 1-2 layers, 5 wheels, 12 sectors
  - Endcap: $2 \times 3$ stations, 2 rings, 36 sectors
  - Local hit per chamber
  - Time resolution $\lesssim 3\,ns$

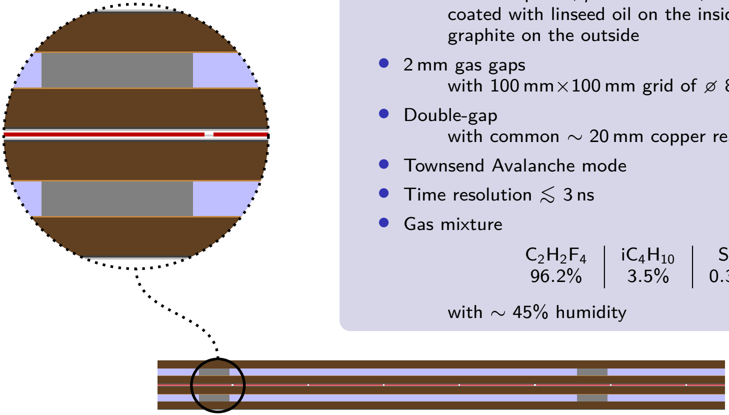

- 2 mm bakelite plates, $\rho \sim 10^{10}\,\Omega\,\mathrm{cm}$,
  coated with linseed oil on the inside,
  graphite on the outside
- 2 mm gas gaps
  with 100 mm × 100 mm grid of ⌀ 8 mm spacers
- Double-gap
  with common ∼ 20 mm copper readout strips
- Townsend Avalanche mode
- Time resolution $\lesssim$ 3 ns
- Gas mixture

| $C_2H_2F_4$ | $iC_4H_{10}$ | $SF_6$ |
|---|---|---|
| 96.2% | 3.5% | 0.3% |

with ∼ 45% humidity

# Outline

# RPC Detector Performance

## RPC Hit Efficiencies

Using CSC and DT segments, RPC efficiencies can be defined without final physics objects
This allows storage of high statistics with low impact on the High Level Trigger

### Segment Extrapolation Method

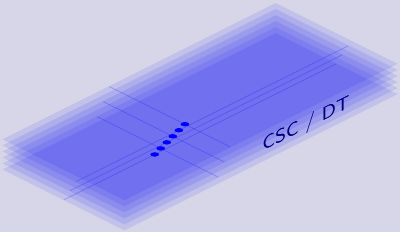

Using CSC and DT segments, RPC efficiencies can be defined without final physics objects
This allows storage of high statistics with low impact on the High Level Trigger

### Segment Extrapolation Method

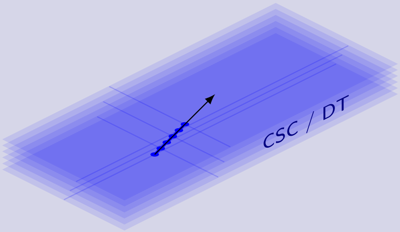

Using CSC and DT segments, RPC efficiencies can be defined without final physics objects
This allows storage of high statistics with low impact on the High Level Trigger

### Segment Extrapolation Method

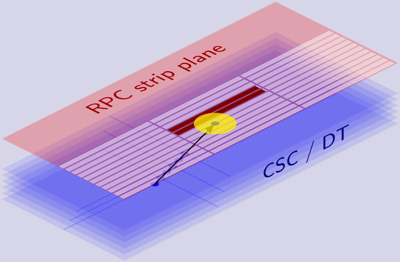

# RPC Detector Performance
## RPC Hit Efficiencies

Using CSC and DT segments, RPC efficiencies can be defined without final physics objects
This allows storage of high statistics with low impact on the High Level Trigger

### Segment Extrapolation Method

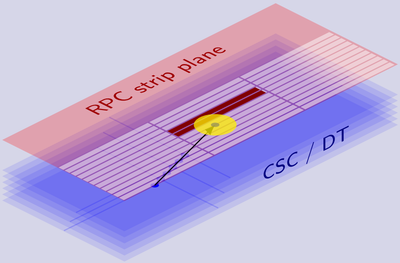


### Hit Efficiency for a single chamber

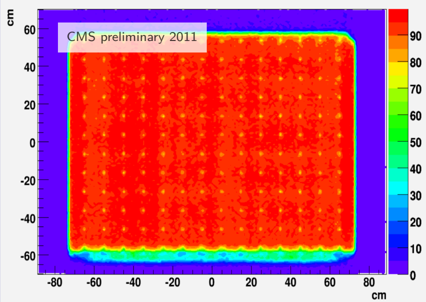

# RPC Detector Performance

## RPC Hit Efficiencies

Using CSC and DT segments, RPC efficiencies can be defined without final physics objects
This allows storage of high statistics with low impact on the High Level Trigger

### Segment Extrapolation Method

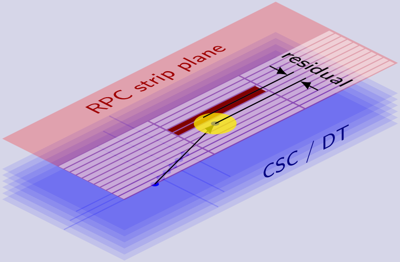


### Hit Efficiency for a single chamber

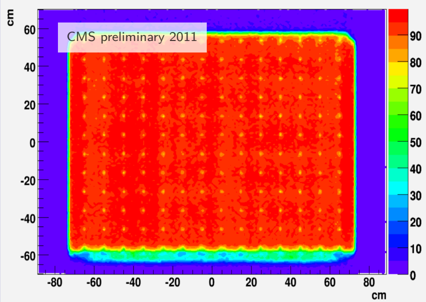

Using the aforementioned residuals, RPC hit resolutions can be defined for the different strip widths throughout the detector

## Residuals for Barrel

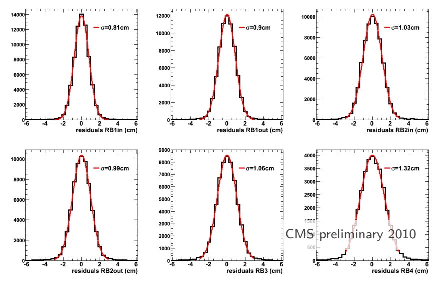


Resolutions range from $\sigma = 0.81$ cm in the inner, to $\sigma = 1.32$ cm in the outer station
Strip widths range from 2.28 cm to 4.10 cm ($\sim \Delta\phi = 18'45''$ )

## Residuals for Endcap

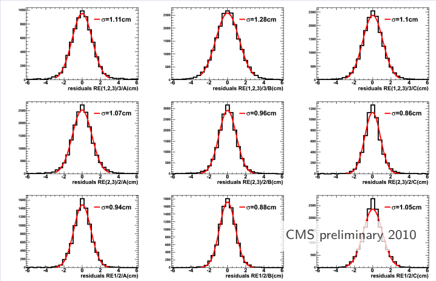


Resolutions range from $\sigma = 0.86$ cm in the inner, to $\sigma = 1.28$ cm in the outer ring
Average strip widths range from 1.95 cm to 3.63 cm ($\sim \Delta\phi = 18'45''$ )

# RPC Detector Performance

## High Voltage Scan 2011

### Typical RPC Chamber

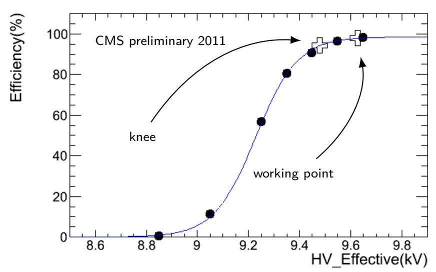


### Goal

- To assure high efficiency
- To minimize pressure and temperature dependency
- To avoid unnecessary stress on the detector
- To avoid increasing clustersize

The avalanche $P$, $T$ and HV dependence can be summarized in $\mathrm{HV_{eff}}$:

$$\mathrm{HV_{eff}} = \mathrm{HV}\frac{P_0}{P}\frac{T}{T_0}$$

$(P_0 = 965\ \mathrm{mbar},\ T_0 = 293\ \mathrm{K})$

# RPC Detector Performance

## High Voltage Scan 2011

### Typical RPC Chamber

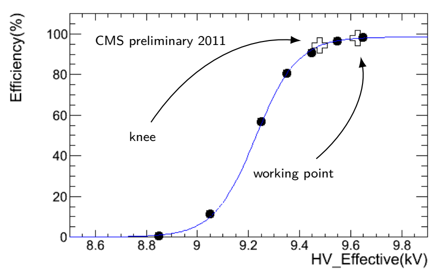


Fitted sigmoidal efficiency curve

$$\epsilon = \frac{\epsilon_{\text{max}}}{1 + e^{s(\text{HV}_{\text{eff}} - \text{HV}_{50\%})}}$$

where $\text{HV}_{50\%}$ is the $\text{HV}_{\text{eff}}$ for which $\epsilon = \frac{\epsilon_{\text{max}}}{2}$

### Goal

- To assure high efficiency
- To minimize pressure and temperature dependency
- To avoid unnecessary stress on the detector
- To avoid increasing clustersize

### Method

- Data was taken at 11 HV points between 8.5 kV and 9.7 kV
- A dedicated data stream provides high statistics in limited time
- A sigmoid was fitted to the measured hit efficiencies per roll
- A working point $\text{HV}_{\text{WP}}$ is defined per chamber

$$\text{HV}_{\text{WP}} = \text{HV}_{\text{knee}} + \begin{cases} 100\,\text{V (barrel)} \\ 150\,\text{V (endcap)} \end{cases}$$

where $\text{HV}_{\text{knee}}$ is the $\text{HV}_{\text{eff}}$ for which efficiency $\epsilon = 0.95 \cdot \epsilon_{\text{max}}$

# RPC Detector Performance

## High Voltage Scan 2011

### Typical RPC Chamber

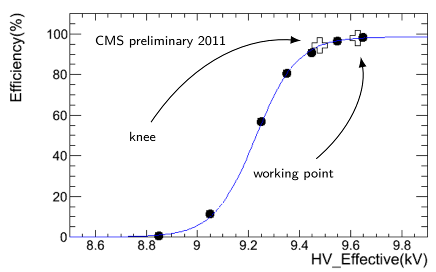


Fitted sigmoidal efficiency curve

$$\epsilon = \frac{\epsilon_{max}}{1 + e^{s(HV_{eff} - HV_{50\%})}}$$

where $HV_{50\%}$ is the $HV_{eff}$ for which $\epsilon = \frac{\epsilon_{max}}{2}$

### $\chi^2$ distribution (11 degrees of freedom)

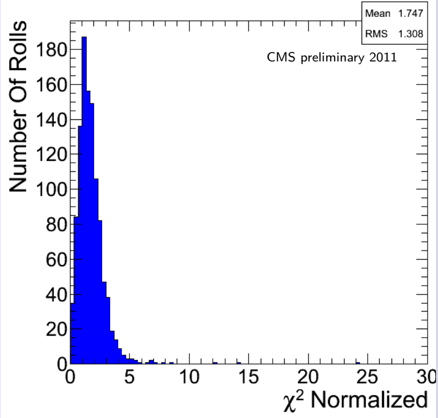


All efficiency curves are nicely sigmoidal in shape

# RPC Detector Performance

## High Voltage Scan 2011

### Typical RPC Chamber

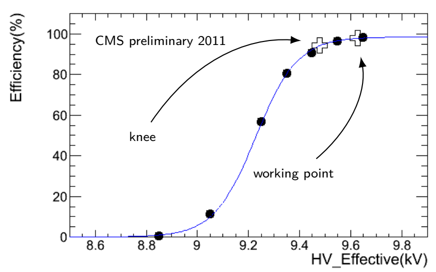


Fitted sigmoidal efficiency curve

$$\epsilon = \frac{\epsilon_{max}}{1 + e^{s(HV_{eff} - HV_{50\%})}}$$

where $HV_{50\%}$ is the $HV_{eff}$ for which $\epsilon = \frac{\epsilon_{max}}{2}$

### Goal

- To assure high efficiency
- To minimize pressure and temperature dependency
- To avoid unnecessary stress on the detector
- To avoid increasing clustersize

### Method

- Data was taken at 11 HV points between 8.5 kV and 9.7 kV
- A dedicated data stream provides high statistics in limited time
- A sigmoid was fitted to the measured hit efficiencies per roll
- A working point $HV_{WP}$ is defined per chamber

$$HV_{WP} = HV_{knee} + \begin{cases} 100\,\text{V (barrel)} \\ 150\,\text{V (endcap)} \end{cases}$$

where $HV_{knee}$ is the $HV_{eff}$ for which efficiency $\epsilon = 0.95 \cdot \epsilon_{max}$

Distribution of the calculated $HV_{working\ point}$

## Barrel

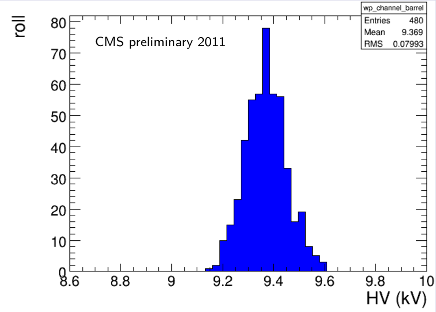


## Endcap

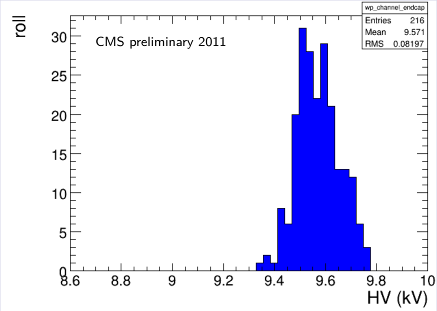


The difference between Barrel and Endcap RPCs comes from a difference in construction techniques
A procedure of averaging is applied since different rolls share a High Voltage supply channel

# RPC Detector Performance
## High Voltage Scan 2011

Measured and predicted hit efficiency for Barrel and Endcap

### Barrel

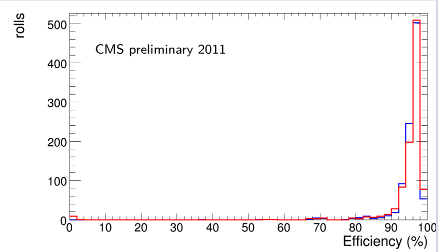


- Predicted Efficiency, $\bar{\epsilon} = 95.2\,\%$, $\mathrm{RMS}_\epsilon = 4.6\,\%$
- Measured Efficiency, $\bar{\epsilon} = 94.4\,\%$, $\mathrm{RMS}_\epsilon = 10.5\,\%$

### Endcap

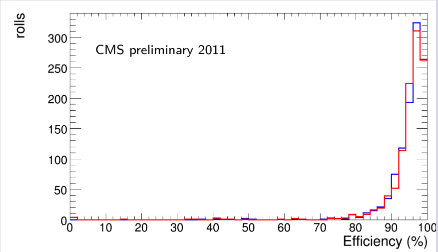


- Predicted Efficiency, $\bar{\epsilon} = 94.7\,\%$, $\mathrm{RMS}_\epsilon = 6.0\,\%$
- Measured Efficiency, $\bar{\epsilon} = 94.2\,\%$, $\mathrm{RMS}_\epsilon = 8.9\,\%$

Prediction from sigmoidal interpolation

# RPC Detector Performance

## High Voltage Scan 2011

### Average hit efficiency for Barrel and Endcap

Remains a 1% efficiency variation due to changes in pressure (CMS Temperature is almost constant)
A pressure correction of the Applied High Voltage has been introduced recently (to be evaluated in the near future)

### Barrel

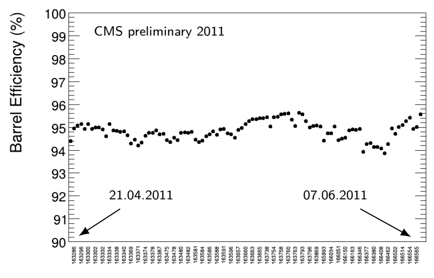


Average Barrel efficiency $\overline{\epsilon} = 94.9\,\% \pm 1.0\,\%$

### Endcap

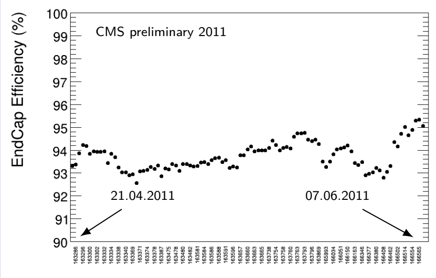


Average Endcap efficiency $\overline{\epsilon} = 93.8\,\% \pm 1.0\,\%$

# RPC Detector Performance

## High Voltage Scan 2011

### Average hit efficiency for Barrel and Endcap

Remains a 1% efficiency variation due to changes in pressure (CMS Temperature is almost constant)
A pressure correction of the Applied High Voltage has been introduced recently (to be evaluated in the near future)

#### Efficiency vs Pressure Barrel

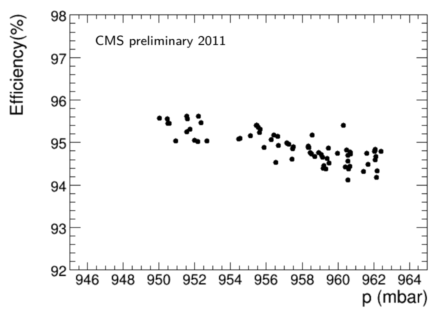


#### Efficiency vs Pressure Endcap

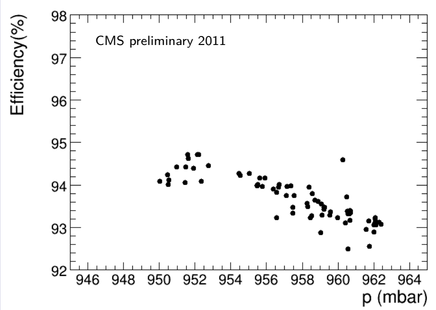

# RPC Detector Performance

## High Voltage Scan 2011

Average cluster size vs $HV_{eff}$

Measured and predicted cluster size at $HV_{working\ point}$

### Typical chamber

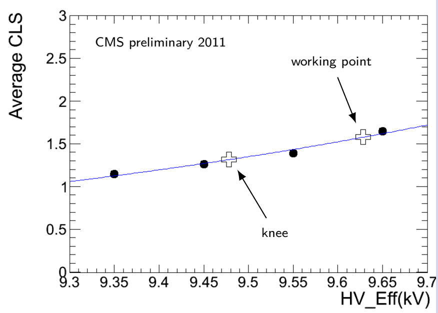


### Cluster size

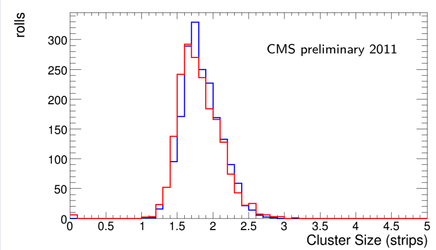


- Predicted Cluster Size, $\overline{CLS} = 1.8, RMS_{CLS} = 0.3$
- Measured Cluster Size, $\overline{CLS} = 1.8, RMS_{CLS} = 0.3$

The cluster size is defined as the number of contiguous strips associated to a hit;
on average it remains within specifications, i.e. below 2 strips (important for trigger algorithm)

# RPC Detector Performance

## High Voltage Scan 2011

Strip noise vs $HV_{eff}$

Measured strip noise at $HV_{working\ point}$

### Typical chamber

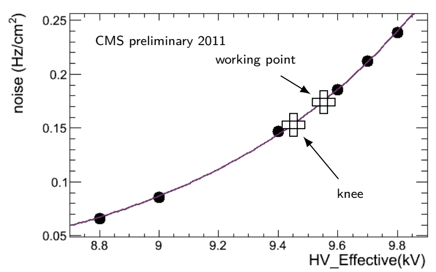


### Endcap

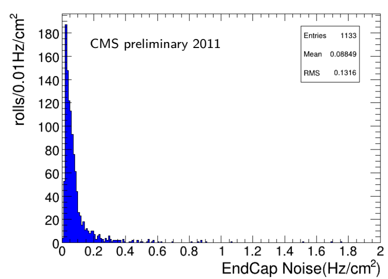


Average noise Barrel and Endcap $\sim 0.08\,\mathrm{Hz\,cm}^{-2}$

The noise is computed measuring hit rates during periods without beam collisions

Most chambers show an intrinsic noise below $0.5\,\mathrm{Hz\,cm}^{-2}$, negligible for accidentals in the trigger system

# Outline

# RPC Trigger Performance

## CMS Trigger system

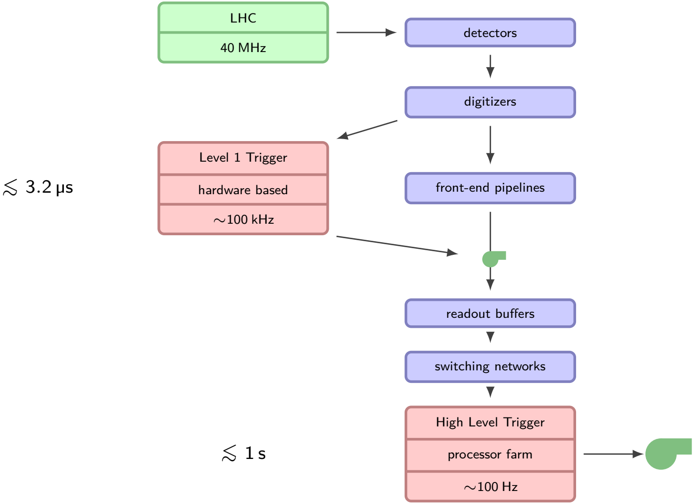

# RPC Trigger Performance
## CMS Trigger system

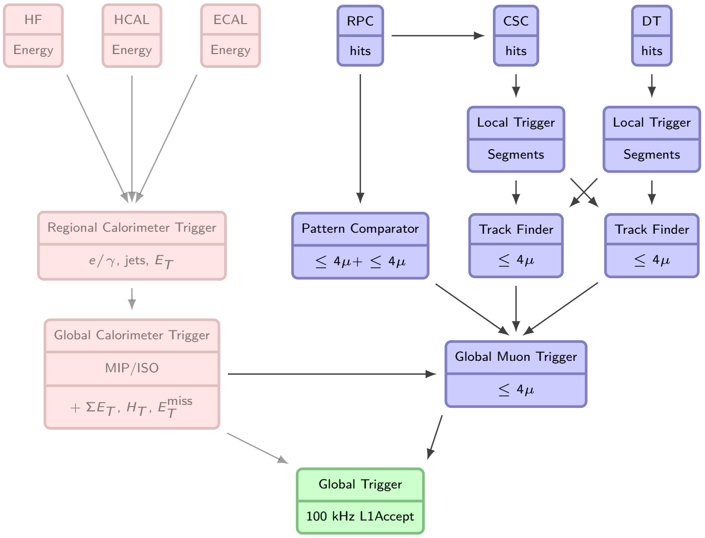

# RPC Trigger
## Pattern Comparator Algorithm

The RPC subdetector is divided in $\eta - \phi$ cones

### $\eta$ segmentation

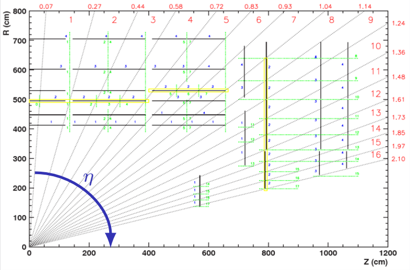


33 towers along $\eta$
3-6 layers per tower

### $\phi$ segmentation

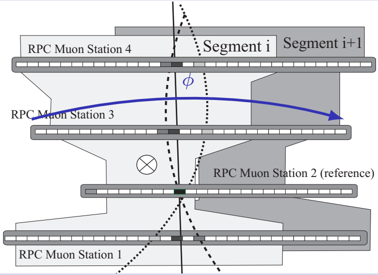


144 segments along $\phi$
ie 8 strips in the reference layer

Hits are matched to Monte Carlo generated patterns in FPGAs
A majority rule defines if a pattern ($\mu$) is found in each cone

- 2010: 4/6 in Barrel, 3/3 in Endcap
- 2011: 3/6 in Barrel, 3/3 in Endcap

A sorting algorithm brings the number back to $\leq 4\mu$ per region (Barrel and Endcap)

## L1 RPC Trigger Efficiency at $\sqrt{s} = 7$ TeV

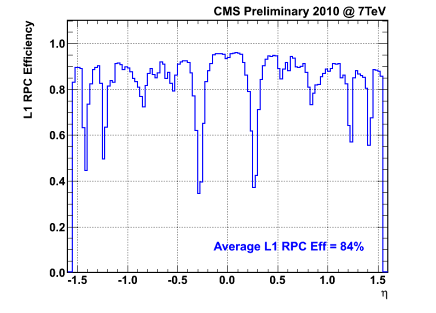


2010 data

- Reconstructed muons with $p_T \geq 7$ GeV/c
- Associated L1 CSC or DT trigger

| Combination of | Approximate contribution to inefficiency | |
|---|---|---|
| | Barrel | Endcap |
| | $(\lvert\eta\rvert < 0.8)$ | $(1.25 < \lvert\eta\rvert < 1.6)$ |
| Geometrical acceptance | 7 % | 8 % |
| Hit efficiency | 6 % | 12 % |
| Intrinsic PAC efficiency | 3 % | <1 % |

(estimation accuracy limited due to track association uncertainty ($\sim$ 1 %))

## L1 RPC Trigger Efficiency at $\sqrt{s} = 7\,\text{TeV}$

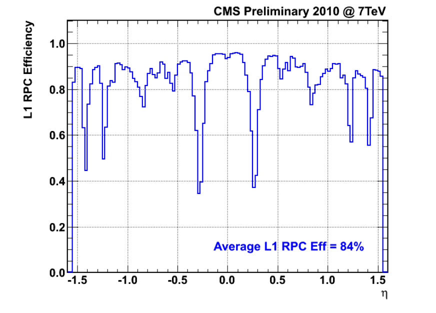


### 2010 data

- Reconstructed muons with $p_T \geq 7\,\text{GeV}/c$
- Associated L1 CSC or DT trigger

### 2011

- Changed majority rule from 4/6 to 3/6 in Barrel
- Improved detector performance

### future

- Addition of the 4th Endcap plane

| Combination of | Approximate contribution to inefficiency | |
|---|---|---|
| | Barrel | Endcap |
| | $(\vert\eta\vert < 0.8)$ | $(1.25 < \vert\eta\vert < 1.6)$ |
| Geometrical acceptance | 7 % | 8 % |
| Hit efficiency | 6 % | 12 % |
| Intrinsic PAC efficiency | 3 % | <1 % |

(estimation accuracy limited due to track association uncertainty ($\sim$ 1 %))

# Outline

# RPC Detector Performance
## Background studies

- Hit counting
  - counted after discriminators
  - no triggers involved
  - hits within 25 ns bunch-crossing window
- Differences in rate
  - inner: HCAL particle leakage
  - outer: slow neutron gas
  - other rings: protected by return yoke
  - azimuthal assymetry due to
    wheel supports
    steel floor

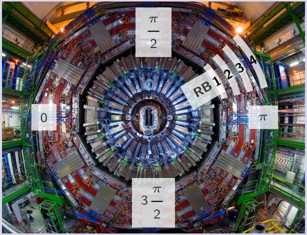


### Barrel $r$ dependence

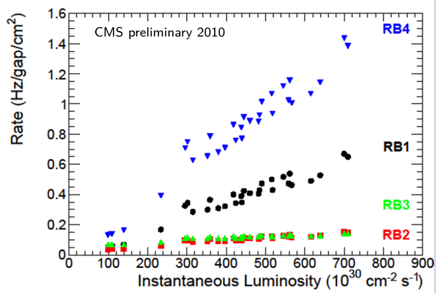

# RPC Detector Performance

## Background studies

- Hit counting
  - counted after discriminators
  - no triggers involved
  - hits within 25 ns bunch-crossing window
- Differences in rate
  - inner: HCAL particle leakage
  - outer: slow neutron gas
  - other rings: protected by return yoke
  - azimuthal assymetry due to
    - wheel supports
    - steel floor

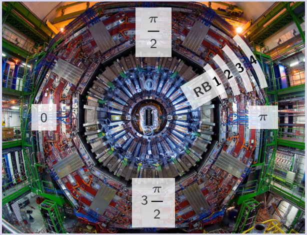


### Barrel $\phi$ assymetry for given run

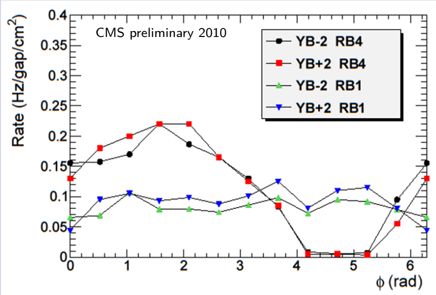


At instantaneous luminosity $1.5 \times 10^{32}\ \mathrm{cm}^{-2}\,\mathrm{s}^{-1}$

# Outline

# Conclusions

- The performance of the CMS RPC subdetector has been investigated in depth
- Both normal and dedicated runs have contributed to a good understanding of the detector
- Resulting measures contributed to its overall efficiency and stability
- The background is being monitored and understood
- The RPCs are ready for further LHC collisions